Comparison between wave functions in the random phase approximation, renormalized random phase approximation, and self-consistent random phase approximation methods

J. G. Hirsch,[1] O. Civitarese,[2] and M. Reboiro[2]
[1]*Instituto de Ciencias Nucleares, Universidad Nacional Autónoma de México, Apartado Postal 70-543, México 04510 Distrito Federal, México*
[2]*Departamento de Física, Universidad Nacional de La Plata, C.C. 67, La Plata (1900), Argentina*
(Received 9 December 1998; published 16 July 1999)

The random phase approximation (RPA), the renormalized RPA (RRPA), and the self-consistent RPA (SCRPA) methods are applied to calculate the wave functions of the ground and excited states of an exactly solvable model. The approximated wave functions are expanded in the basis of the exact solutions. It is found that, when the RPA collapses, the RPA wave functions are orthogonal to the exact solutions while the RRPA and SCRPA ones have small but finite overlaps with the exact results. In spite of the apparently good agreement between the results of the RRPA, the SCRPA, and the exact solution, for the energy of the first excited state beyond the point of collapse, it is found that these approximations do not correctly describe the exact wave functions. [S0556-2813(99)03808-X]

PACS number(s): 21.60.Jz, 21.60.Fw

Various generalizations of the random-phase approximation (RPA) have been reported recently [1–4]. The renormalized RPA (RRPA) is the simplest of these approximations and it aims at a better treatment of ground-state correlations, as compared with the RPA method. As shown in [3,4] the RRPA results go beyond the collapse of the RPA [3,4]. The self-consistent RPA (SCRPA) [5,6] is a more sophisticated approximation which avoids the collapse by introducing the coupling between one-particle and particle-hole density fluctuations. Results of the SCRPA treatment of realistic nuclear interactions can be found in [7].

The properties and limitations of the RPA and related approximations, for the case of exactly solvable models, were studied long ago [8]. Excitation energies, transition matrix elements, and sum rules have been the observables of choice, in assessing the validity of the RPA [8]. Concerning wave functions, the exactly solvable Lipkin model [9] has been used to compare exact and RPA ground-state wave functions and correlations.

In the present work we report on the results which we have obtained by using the Lipkin model to build the wave function of excited states and to expand the RPA wave functions in terms of the exact solutions. The same is done for the cases of the RRPA and SCRPA. The comparison between the wave functions obtained within these approximations and the exact ones is discussed in order to assess the validity of the methods.

The model Hamiltonian is taken from [9] and it reads

$$H=\epsilon J_0-\frac{V}{2}(J_+^2+J_-^2), \tag{1}$$

where

$$J_0=\frac{1}{2}\sum_{m=1}^{2\Omega}(c_{1m}^\dagger c_{1m}-c_{0m}^\dagger c_{0m}),\quad J_+=\sum_{m=1}^{2\Omega}c_{1m}^\dagger c_{0m},$$

$$J_-=\sum_{m=1}^{2\Omega}c_{0m}^\dagger c_{1m} \tag{2}$$

are the number and the particle-hole operators, respectively. The indices 0 and 1 denote the lower and upper single-particle levels, with energies $\epsilon_{0(1)}=\mp\epsilon/2$, ϵ being the energy spacing between levels, and m is the internal quantum number (i.e., the angular momentum projection) which varies between $1\rightarrow 2\Omega$ for each shell. These operators are the generators of the algebra of the SU(2) group. The number of particles is $N=2\Omega$, and V is the strength of the interaction. Exact eigenvalues and eigenvectors of the Hamiltonian H, of Eq. (1), are obtained in the basis

$$|n\rangle=\sqrt{\frac{(2\Omega-n)!}{n!(2\Omega)!}}J_+^n|\rangle. \tag{3}$$

The state $|\rangle$ is the unperturbed ground state. For this case all the particles occupy the lowest single-particle state and it implies $J_0|\rangle=-\Omega|\rangle$. Since the Hamiltonian of Eq. (1) has nonvanishing matrix elements between states (3) with $n\rightarrow n,n\pm 2$ its eigenfunctions can be written in terms of linear combinations of states with even (e) or odd (o) values of n (e.g., the number of particle-hole pairs), namely,

$$|\lambda,e\rangle=\sum_{n=0}^{\Omega}C_{n,e}^{\lambda}|2n\rangle,\quad |\lambda,o\rangle=\sum_{n=0}^{\Omega-1}C_{n,o}^{\lambda}|2n+1\rangle. \tag{4}$$

In this notation λ is the eigenvalue index, thus $|\lambda=1,e\rangle$ and $|\lambda=1,o\rangle$ are the exact ground state and the exact first excited state, respectively.

In the following we shall describe the main steps of the equation of motion method [2] (EOM). The starting point of the EOM is the definition of the one-phonon state created by the action of the phonon creation operator $\Gamma^\dagger$ on the correlated vacuum $|0\rangle$,

$$|n_{\text{phonon}}=1\rangle=\Gamma^\dagger|0\rangle. \tag{5}$$

 ©1999 The American Physical Society

This vacuum is defined by the condition $\Gamma|0\rangle=0$, where the one-phonon annihilation operator Γ is the adjoint of $\Gamma^\dagger$. The true eigenstates of H can be described, approximately, by the one-phonon states $|k\rangle=\Gamma_k^\dagger|0\rangle$ after solving the EOM equations. The structure of the wave function of each one-phonon state $|k\rangle$ can be determined from a variation [2] and it can be shown from the previous equations that

$$\langle 0|[\delta\Gamma_k,H,\Gamma_k^\dagger]|0\rangle=\omega_k\langle 0|[\delta\Gamma_k,\Gamma_k^\dagger]|0\rangle \tag{6}$$

with

$$2\langle 0|[\delta\Gamma_k,H,\Gamma_k^\dagger]|0\rangle=\langle 0|[\delta\Gamma_k,[H,\Gamma_k^\dagger]]|0\rangle + \langle 0|[[\delta\Gamma_k,H],\Gamma_k^\dagger]|0\rangle, \tag{7}$$

where ω_k is the kth eigenvalue and $\delta\Gamma_k$ is an arbitrary variation of the kth eigenfunction.

The main assumption of the random phase approximation (RPA) is that the one-phonon creation operator is built as a linear combination of particle-hole operators (J_+,J_-). In the Lipkin model, Hamiltonian (1), there is only one of such phonons and it is written as

$$\Gamma^\dagger=\frac{1}{\sqrt{2\Omega}}(XJ_+-YJ_-). \tag{8}$$

By using in Eq. (6) the above definition, the usual RPA matrix equations [2,8] are obtained

$$\begin{pmatrix} A & B \\ -B & -A \end{pmatrix}\begin{pmatrix} X \\ Y \end{pmatrix}=\omega U\begin{pmatrix} X \\ Y \end{pmatrix}. \tag{9}$$

The quantities A, B, and U are defined by

$$A=\langle 0|[J_-,H,J_+]|0\rangle,\quad B=-\langle 0|[J_-,H,J_-]|0\rangle,$$
$$U=\langle 0|[J_-,J_+]|0\rangle. \tag{10}$$

The forward- and backward-going RPA amplitudes X and Y are normalized as

$$\langle 0|\Gamma\Gamma^\dagger|0\rangle=\langle 0|[\Gamma,\Gamma^\dagger]|0\rangle=(X^2-Y^2)\frac{\langle 0|-2J_0|0\rangle}{2\Omega}. \tag{11}$$

Furthermore, it is assumed that

$$X^2-Y^2=1. \tag{12}$$

The standard RPA matrix elements A and B of the Eq. (9) are obtained by assuming $|0\rangle\approx|\rangle$, and consequently that $\langle 0|J_0|0\rangle\approx\langle|J_0|\rangle=-\Omega$, and

$$A_{\rm RPA}=\epsilon,\quad B_{\rm RPA}=-(2\Omega-1)V\approx-2\Omega V. \tag{13}$$

The RPA excitation energy ω [8] is given by $\omega=\sqrt{\epsilon^2-4\Omega^2V^2}$, and it vanishes if $V=\epsilon/(2\Omega)$. Under the above conditions the so-called *quasiboson approximation*

$$\langle 0|\Gamma\Gamma^\dagger|0\rangle=1 \tag{14}$$

is fulfilled. It is valid except for the strong-coupling limit since for large values of the strength V $[V\to\epsilon/(2\Omega)]$ the RPA amplitudes X and Y diverge and $\langle 0|-2J_0|0\rangle\to 0$. Obviously the RPA eigenstate is not normalizable in the strong-coupling situation.

In the self-consistent RPA (SCRPA) approach [6,10], the expressions (8) and the Hermitian conjugate are inverted giving J_+ and J_- in terms of $\Gamma^\dagger$ and Γ. By replacing the particle-hole operators $J_\pm$ by phonon operators and enforcing the constraint $\Gamma|0\rangle=0$, one gets the matrix elements A and B of Eq. (9) in the form

$$A_{\rm SCRPA}=\epsilon+2VXY,$$
$$B_{\rm SCRPA}=2\frac{\langle 0|J_0^2|0\rangle}{\langle 0|J_0|0\rangle}V+V(X^2+Y^2). \tag{15}$$

There are two unknown quantities in $B_{\rm SCRPA}$, they are $\langle 0|J_0^2|0\rangle$ and $\langle 0|J_0|0\rangle$. The simplest approximation which can be applied to determine them is the following:

$$\frac{\langle 0|J_0^2|0\rangle}{\langle 0|J_0|0\rangle}\approx-\Omega. \tag{16}$$

After performing this approximation it is seen that Eq. (15) differs from Eq. (13) mainly in the term added to the forward matrix A. Notice that the particle-hole unperturbed energy ϵ is the only contribution to the forward matrix which appears in the Lipkin model. If we take the limit $Y\to 0$ in Eq. (15), then Eq. (13) is recovered.

If the approximation

$$\frac{\langle 0|J_0^2|0\rangle}{\langle 0|J_0|0\rangle}\approx\langle 0|J_0|0\rangle \tag{17}$$

is used instead of Eq. (16) and the weak interaction limit $Y\to 0$ is enforced, then the renormalized RPA matrices are obtained [3]:

$$A_{\rm RRPA}=\epsilon,\quad B_{\rm RRPA}=-2\Omega VD. \tag{18}$$

The renormalization factor D, which allows for a proper normalization of the eigenvectors in Eq. (11), is defined as

$$D\equiv\langle 0|\Gamma\Gamma^\dagger|0\rangle=\frac{\langle 0|-2J_0|0\rangle}{2\Omega}. \tag{19}$$

Different expressions for D as a function of Y^2 can be found in the literature [1,3,4]. Among them the most frequently used is the one due to Catara *et al.* [3,4], where D is defined as

$$D=\frac{1}{1+Y^2/\Omega}. \tag{20}$$

We shall now discuss the structure of the wave functions, as they are given by each of the above introduced approximations. The RPA ground state is given by [2,6,9,10]

$$|0\rangle=\mathcal{N}^{-1}\sum_{l=0}^{\Omega}\frac{(2\Omega-2l)!}{(\Omega-l)!l!}\left(\frac{Y}{X}\right)^2 J_+^{2l}|\rangle, \tag{21}$$

where

$$\mathcal{N}^2=(2\Omega)!\sum_{l=0}^{\Omega}\left(\frac{Y}{X}\right)^{2l}\frac{(2\Omega-2l)!(2l)!}{(\Omega-l)!^2 l!^2} \tag{22}$$

is the normalization factor. By expanding these wave functions in the basis (4) one gets

$$|0\rangle=\sum_{\lambda}\langle\lambda,e|0\rangle|\lambda,e\rangle. \tag{23}$$

The coefficients $\langle\lambda,e|0\rangle$ are the overlaps between the exact and RPA wave functions and they are given by

$$\langle\lambda,e|0\rangle=\frac{\sqrt{(2\Omega)!}}{\mathcal{N}}\sum_{l=0}^{\Omega}C_{l,e}^{\lambda}\left(\frac{Y}{X}\right)^l\frac{\sqrt{(2\Omega-2l)!(2l)!}}{(\Omega-l)!l!}. \tag{24}$$

By using Eq. (9) the wave function of the RPA excited state takes the form

$$\Gamma^\dagger|0\rangle=\frac{1}{X\sqrt{2\Omega}\sqrt{\langle 0|\Gamma\Gamma^\dagger|0\rangle}}J_+|0\rangle, \tag{25}$$

and its overlap with the exact solutions is expressed by

$$\begin{aligned}\langle\lambda,o|\Gamma^\dagger|0\rangle=&\frac{\sqrt{(2\Omega-1)!}}{X\mathcal{N}\sqrt{\langle 0|\Gamma\Gamma^\dagger|0\rangle}}\\&\times\sum_{l=0}^{\Omega-1}C_{l,o}^{\lambda}\left(\frac{Y}{X}\right)^l\frac{\sqrt{(2\Omega-2l)!(2l+1)!}}{(\Omega-l)!l!}\\&\times\sqrt{2(\Omega-l)}.\end{aligned} \tag{26}$$

Instead of the usual quasiboson approximation, e.g., $\langle 0|\Gamma\Gamma^\dagger|0\rangle=1$, the constraints

$$\sum_{\lambda}|\langle\lambda,e|0\rangle|^2=1,\quad\sum_{\lambda}|\langle\lambda,o|\Gamma^\dagger|0\rangle|^2=1, \tag{27}$$

can be used to determine the normalization factor $\mathcal{N}$ of Eq. (21), which is written in terms of the RPA expectation values of J_0 [6], namely,

$$\langle 0|J_0|0\rangle=\mathcal{N}^{-1}\sum_{l=0}^{\Omega}\left(\frac{Y}{X}\right)^{2l}(2l-\Omega)\frac{(2\Omega-2l)!(2l)!}{(\Omega-l)!^2 l!^2}. \tag{28}$$

The same procedure can be applied to calculate overlaps between exact and RRPA and SCRPA wave functions. As shown above, for the case of the RPA, the matrix equation (10) was solved for the RRPA and SCRPA methods. We have computed the corresponding wave functions and written them in the basis of the exact solutions. Details are omitted for the sake of brevity.

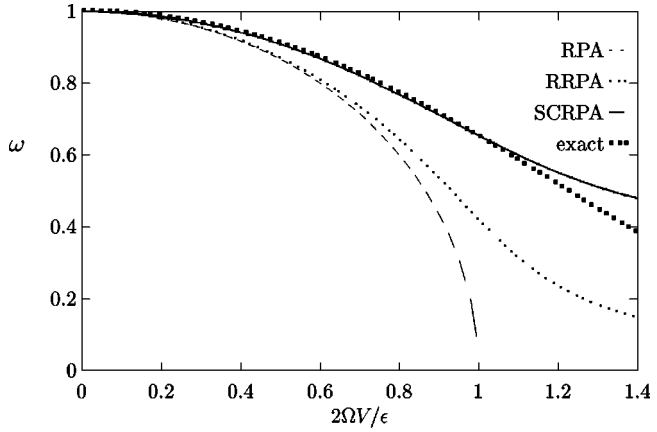

FIG. 1. Excitation energy ω as a function of the reduced interaction strength $2\Omega V/\epsilon$. The upper curves (solid line and large dots) represent SCRPA and exact solutions, respectively. Lower curves (small dots and dashed lines) represent RRPA and RPA results, respectively.

In the following we shall present and discuss results corresponding to the case $\Omega=7$ and $N=2\Omega$ particles. The reduced coupling $2\Omega V/\epsilon$ will be taken as a free parameter varying between 0 and 1.4. This interval includes the weak and the strong-coupling limits as well as the value which produces the collapse of the RPA ($2\Omega V/\epsilon=1$).

Figure 1 shows the comparison between exact and ap-

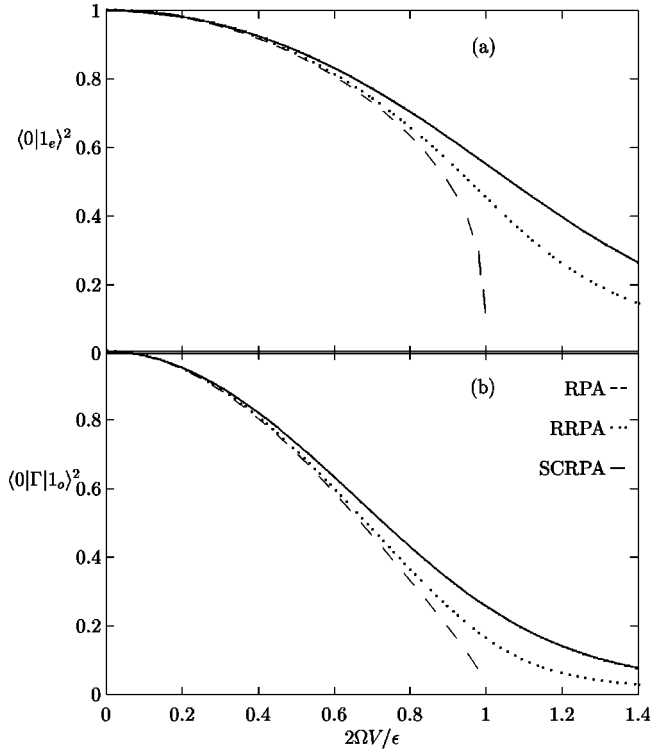

FIG. 2. Overlaps between the exact and RPA, RRPA, and SCRPA wave functions. Insets (a) and (b) show overlaps with the exact ground state ($|1,e\rangle$) and with the exact first excited state ($|1,o\rangle$), respectively. The lines follow the same convention as in Fig. 1.

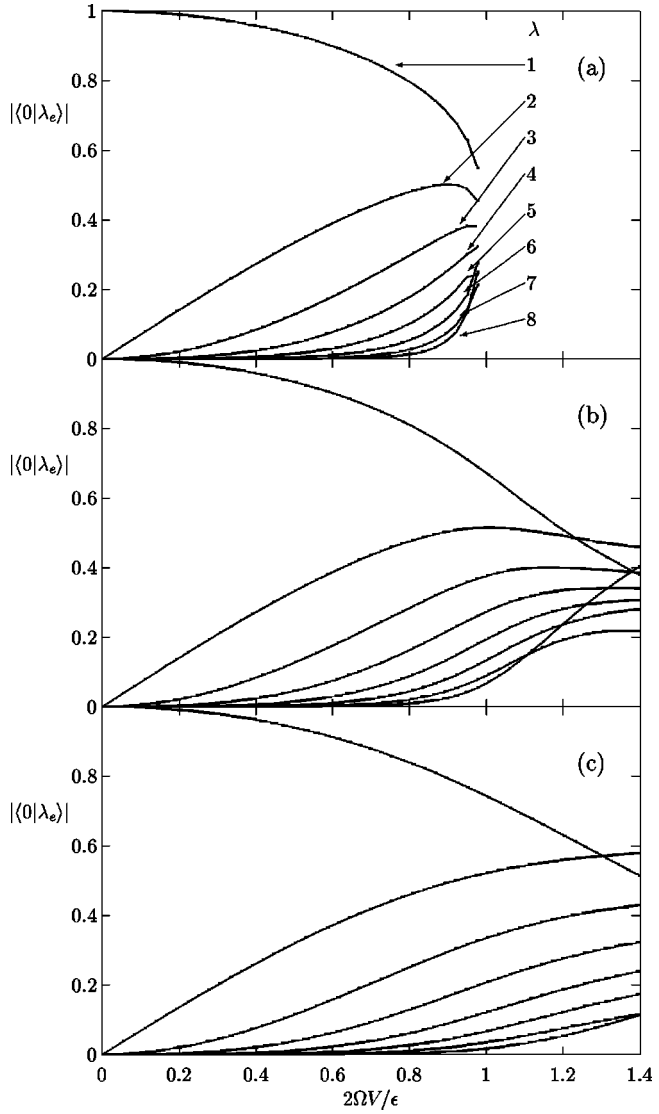

FIG. 3. Amplitudes of the approximated ground state ($|0\rangle$) on the exact solutions ($|\lambda,e\rangle$), as a function of the reduced coupling strength $2\Omega V/\epsilon$. Insets (a), (b), and (c) correspond to RPA, RRPA, and SCRPA ground-state wave functions, respectively. The curves are denoted by $\lambda=1-8$, spanning the eight eigenstates in the model space with $\Omega=7$ and an even number of particle-hole excitations, see Eq. (4). The eigenvalue index λ is explicitly written in the inset (a), for the RPA amplitudes, and the same ordering (from top to bottom) is understood for the curves of the insets (b) and (c).

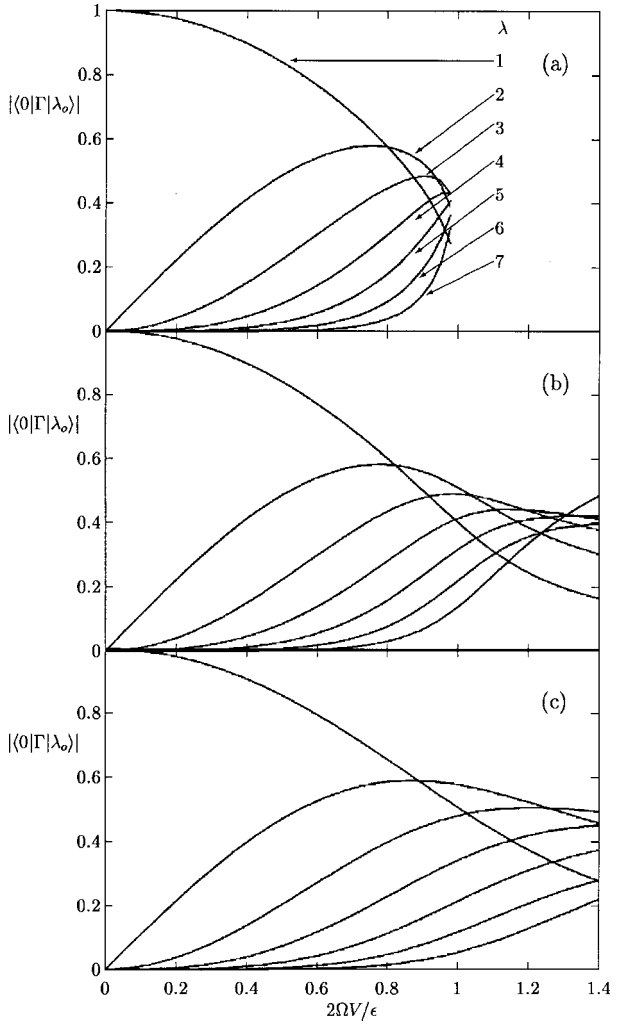

FIG. 4. Amplitudes of the approximated first excited state ($\Gamma^{+}|0\rangle$) on the exact solutions ($|\lambda,o\rangle$), as a function of the reduced coupling strength $2\Omega V/\epsilon$. Insets (a), (b), and (c) show the results corresponding to RPA, RRPA, and SCRPA ground-state wave functions, respectively. The curves are denoted by $\lambda=1$ to 7, spanning the seven eigenstates in the model space with $\Omega=7$ and odd number of particle-hole excitations, see Eq. (4). The ordering of the curves is the same as Fig. 3.

proximated values of the energy of the first excited state ω as a function of the reduced coupling strength defined above. This figure shows already well-known features of the approximations, namely, (i) the collapse of the RPA at $2\Omega V/\epsilon=1$, (ii) the continuation of the RRPA values beyond this point, and (iii) the good agreement between the SCRPA and the exact results for values of $2\Omega V/\epsilon>1$ [3,8,11,10].

Figure 2, case (a), shows the overlaps between the exact ground state and the approximated ones, and Fig. 2, case (b), displays the overlap between the exact first excited state and the approximated ones, calculated by using the different approximations discussed above. At first view the curves shown of Fig. 2 show similar results for small values of the reduced coupling. While the RPA overlaps vanish at $2\Omega V/\epsilon=1$, the RRPA and the SCRPA values decrease steadily beyond this point. In spite of the trend exhibited by the excitation energy (see Fig. 1) the agreement between SCRPA and RRPA wave functions with respect to the exact ones is definitively poor. The discrepancy between the exact wave functions and the approximated ones is simply too large and therefore the applicability of the RRPA and SCRPA beyond the point where the RPA collapses becomes dubious. The RRPA and SCRPA wave functions always keep a finite overlap with the exact solution, but it is decreasing fast after the point where the RPA collapses. Notice that the overlaps shown in case (b) (first excited state) are smaller than the values corresponding to the ground state [case (a) of Fig. 2]. None of the surviving RRPA and SCRPA overlaps, beyond the collapse of the RPA, exceed 50%, case (a), or

30%, case (b). These results are indicative of the discrepancies existing between the exact wave functions and the approximated ones. Also, these discrepancies are affecting the expectation values and the sum rules of transition operators expanded in the same basis (see [11]).

In order to complete the discussion about the comparison between exact and approximated wave functions we have calculated the amplitudes of the RPA, RRPA, and SCRPA wave functions expanded in the complete set of exact solutions. The results are shown in Figs. 3 and 4 for the amplitudes of the approximated ground states and first excited states, respectively.

In Fig. 3 the amplitudes of the RPA ground-state components ($|\langle \lambda, e|0\rangle|$) are presented as functions of the residual interaction strength. As shown in this figure the mixing between the lowest two eigenstates increases as the interaction strength increases, therefore the structure of the approximated ground states changes strongly at each side of the point where the RPA collapses.

Figure 4 displays similar results for the amplitudes of the RPA, RRPA, and SCRPA components of the first excited state ($|\langle \lambda, o|\Gamma^{\dagger}|0\rangle|$). In this case the mixing is larger than for the ground state (see Fig. 3) and the exact first excited state ceases to represent the dominant component of the approximated ones *before* the point of collapse. Beyond that point, there are many other exact states which exhibit sizable overlaps with the RRPA and SCRPA states.

To summarize, we have shown that the RPA wave functions are orthogonal to the exact wave functions if the value of the reduced interaction strength lies near unity, which is the point where the RPA collapses. It is also found that the RRPA and SCRPA methods, which go beyond the point of the RPA collapse, fail badly in reproducing exact eigenfunctions. By using these approximations one obtains finite overlaps with the exact solutions. In spite of the fact that the agreement between the exact and the RRPA and SCRPA values, of the energy for the first excited state past the point of collapse, is not bad, the results for the wave functions show the presence of a strong mixing. These results can be expressed in the shell model language by saying that multiple particle-hole excitations play a non-negligible role in building up correlations nearby the RPA collapse. At least in the case of the schematic model situation which we have discussed, it can be said that neither the RRPA nor the SCRPA are suitable approximations to be used nearby the point of collapse of the RPA. While some of the reported features were already known for the case of the RRPA [11], the results on the SCRPA contribute new evidence about the validity of the method. Particularly the poor agreement between the exact and SCRPA wave functions gives us a signal about the use of the SCRPA in realistic situations.

This work was supported in part by the Conacyt (México) and by Grant No. PICT0079 of the ANPCyT (Argentina). J.G.H. is on a sabbatical leave from the Departamento de Física of the Centro de Investigación y de Estudios Avanzados, México. O.C. and M.R. acknowledge the support of CONICET, Argentina.

[1] K. Hara, Prog. Theor. Phys. **32**, 88 (1964).
[2] D. J. Rowe, Phys. Rev. **175**, 1283 (1968).
[3] F. Catara, N. Dinh Dang, and M. Sambataro, Nucl. Phys. **A579**, 1 (1994).
[4] F. Catara, G. Piccitto, M. Sambataro, and N. Van Giai, Phys. Rev. B **54**, 17 536 (1996).
[5] P. Schuck and S. Ethofer, Nucl. Phys. **A212**, 269 (1973).
[6] J. Dukelsky and P. Schuck, Nucl. Phys. **A512**, 466 (1990).
[7] A. A. Raduta, C. M. Raduta, Amand Faessler, and W. A. Kamiński, Nucl. Phys. **A634**, 497 (1998); A. Bobyk, W. A. Kamińsky, and P. Zareba, nucl-th/9806016.
[8] J. C. Parick and D. J. Rowe, Phys. Rev. **175**, 1293 (1968).
[9] H. J. Lipkin, N. Meshkov, and A. J. Glick, Nucl. Phys. **62**, 188 (1965); **62**, 199 (1965); **62**, 211 (1965).
[10] J. Dukelsky and P. Schuck, Rev. Mex. Fis. **44**, 55 (1998).
[11] O. Civitarese and M. Reboiro, Phys. Rev. C **57**, 3062 (1998).